2-D Impulse and Sifting Property

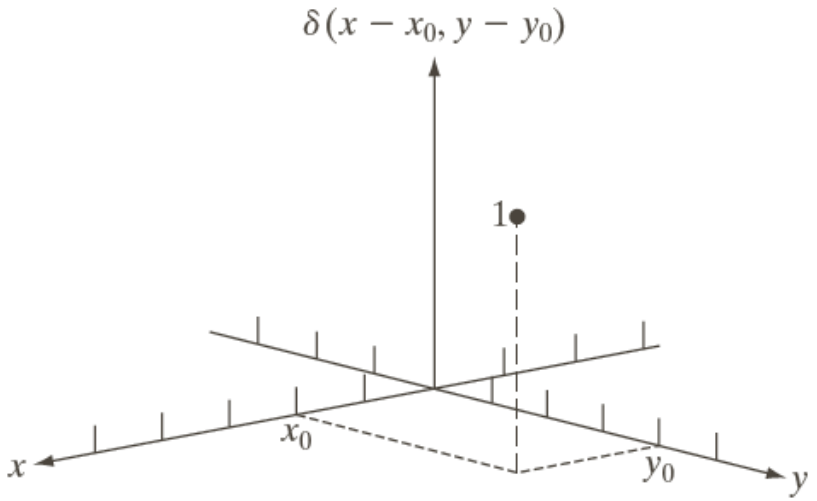

FIGURE 4.12 Two-dimensional unit discrete impulse. Variables x and y are discrete, and δ is zero everywhere except at coordinates (x_0, y_0).

2-D Fourier Transform

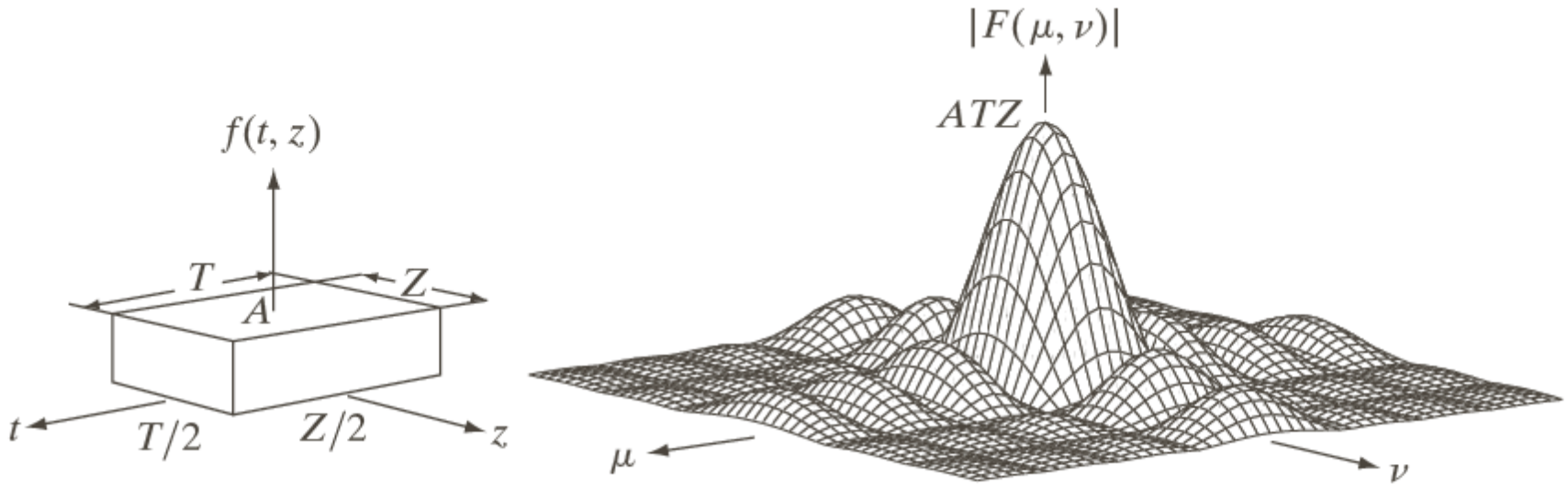

a b

FIGURE 4.13 (a) A 2-D function, and (b) a section of its spectrum (not to scale). The block is longer along the t-axis, so the spectrum is more "contracted" along the μ-axis. Compare with Fig. 4.4.

2-D sampling and Aliasing

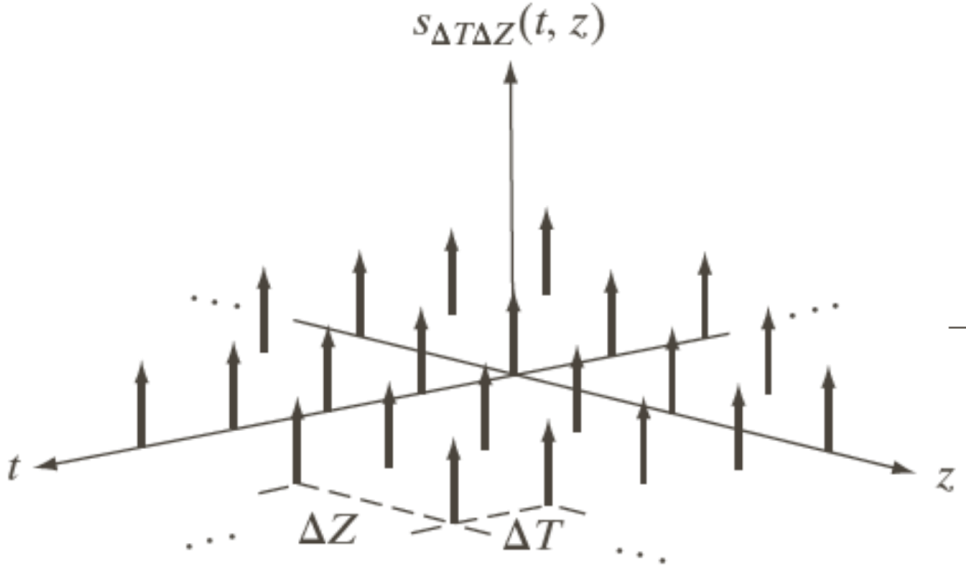

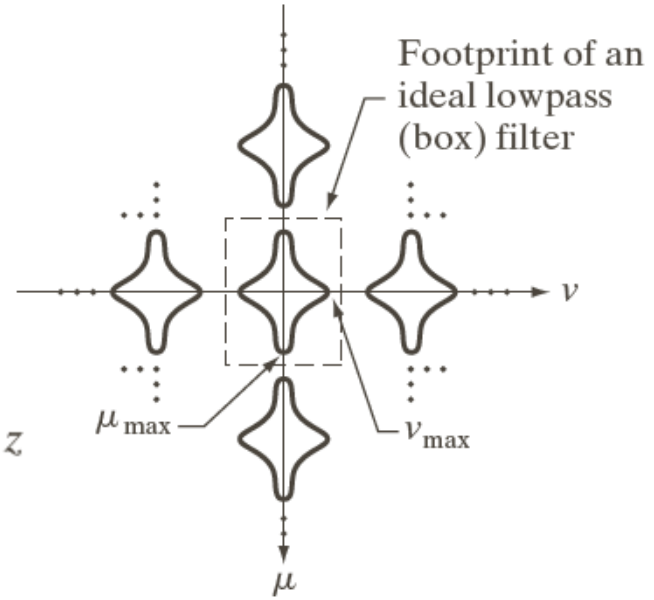

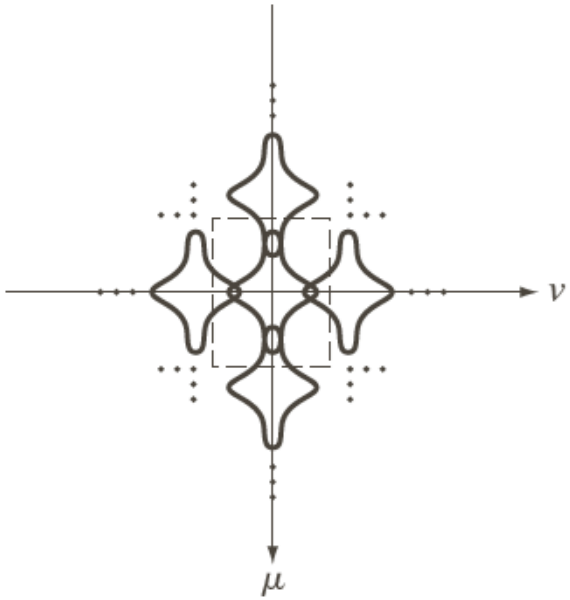

a b

FIGURE 4.15 Two-dimensional Fourier transforms of (a) an over-sampled, and (b) under-sampled band-limited function.

Example of Aliasing

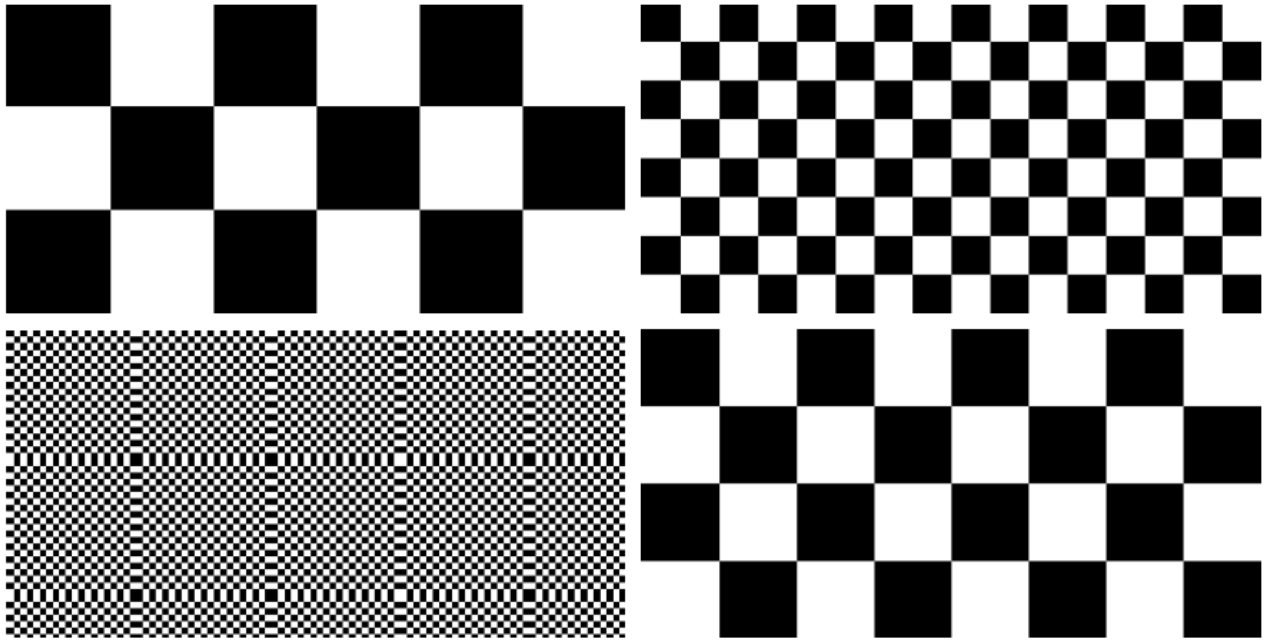

a b
c d

FIGURE 4.16 Aliasing in images. In (a) and (b), the lengths of the sides of the squares are 16 and 6 pixels, respectively, and aliasing is visually negligible. In (c) and (d), the sides of the squares are 0.9174 and 0.4798 pixels, respectively, and the results show significant aliasing. Note that (d) masquerades as a "normal" image.

Temporal Aliasing

Anti-aliasing

a b c

FIGURE 4.17 Illustration of aliasing on resampled images. (a) A digital image with negligible visual aliasing. (b) Result of resizing the image to 50% of its original size by pixel deletion. Aliasing is clearly visible. (c) Result of blurring the image in (a) with a 3×3 averaging filter prior to resizing. The image is slightly more blurred than (b), but aliasing is not longer objectionable. (Original image courtesy of the Signal Compression Laboratory, University of California, Santa Barbara.)

2-D DFT and Periodicity Property

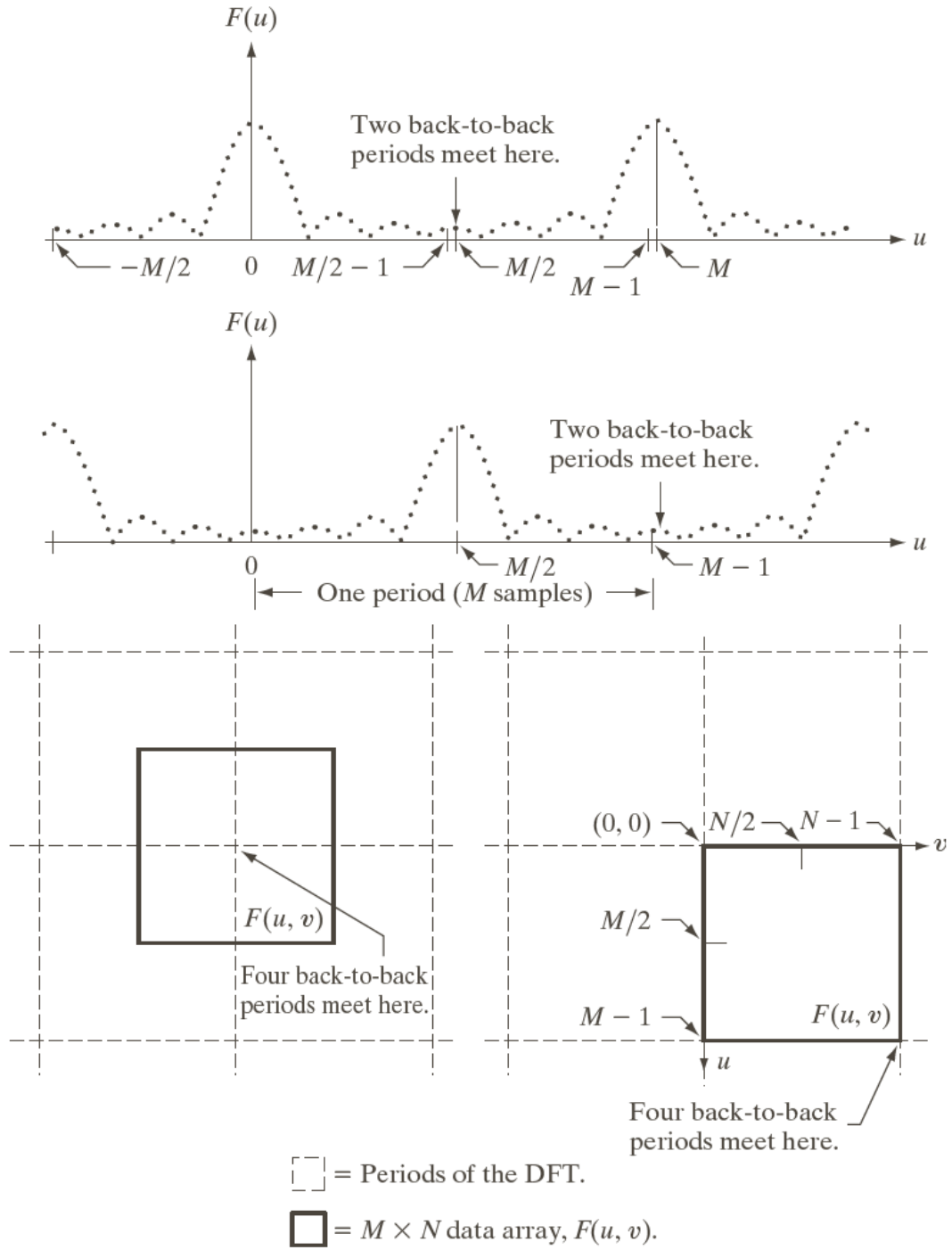

a
b
c d

FIGURE 4.23 Centering the Fourier transform. (a) A 1-D DFT showing an infinite number of periods. (b) Shifted DFT obtained by multiplying $f(x)$ by $(-1)^x$ before computing $F(u)$. (c) A 2-D DFT showing an infinite number of periods. The solid area is the $M \times N$ data array, $F(u, v)$, obtained with Eq. (4.5-15). This array consists of four quarter periods. (d) A Shifted DFT obtained by multiplying $f(x, y)$ by $(-1)^{x+y}$ before computing $F(u, v)$. The data now contains one complete, centered period, as in (b).

Fourier Spectrum and Phase

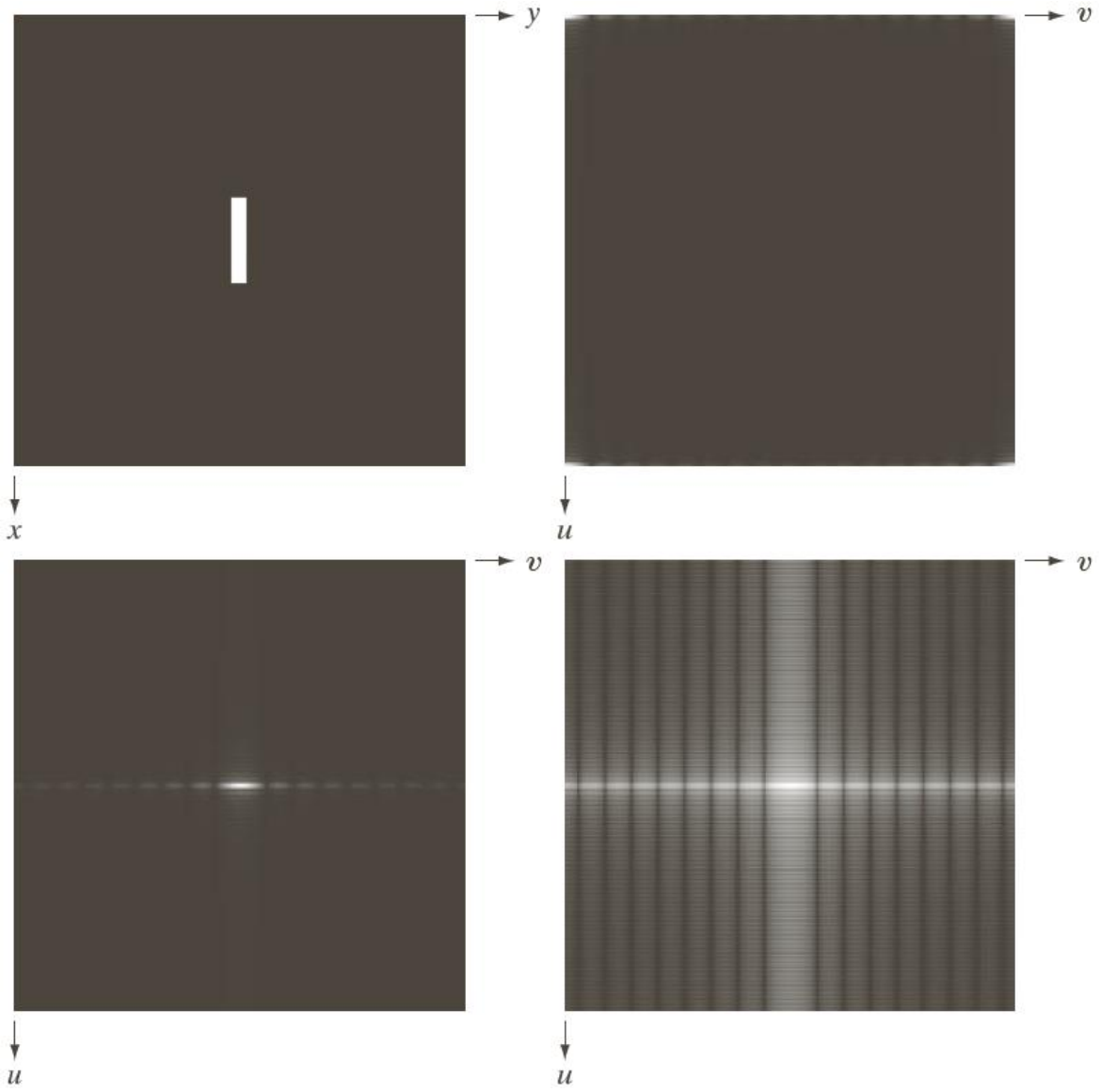

a b
c d

FIGURE 4.24
(a) Image.
(b) Spectrum showing bright spots in the four corners.
(c) Centered spectrum. (d) Result showing increased detail after a log transformation. The zero crossings of the spectrum are closer in the vertical direction because the rectangle in (a) is longer in that direction. The coordinate convention used throughout the book places the origin of the spatial and frequency domains at the top left.

Fourier Spectrum and Phase (contd..)

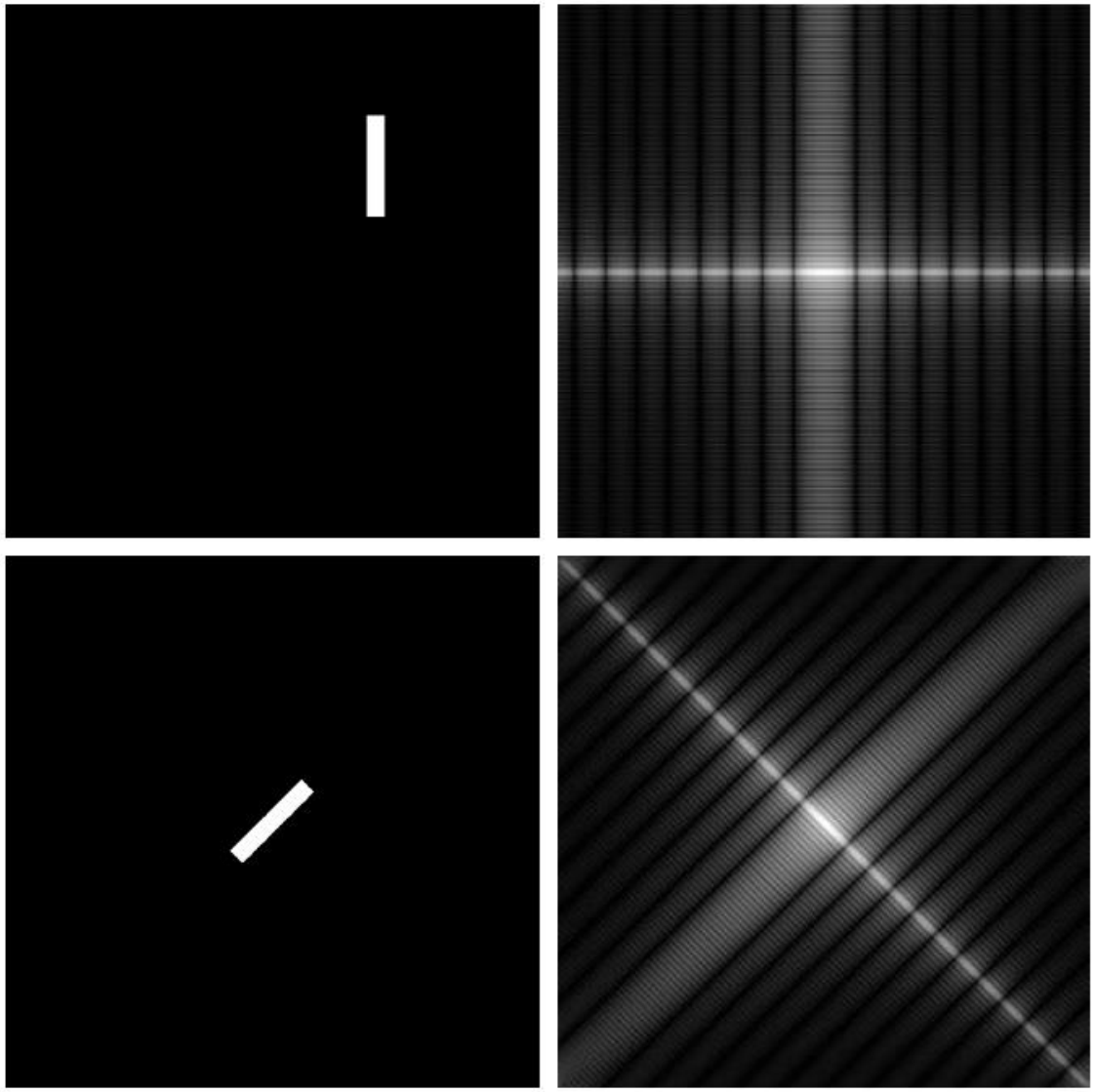

a b
c d

FIGURE 4.25
(a) The rectangle in Fig. 4.24(a) translated, and (b) the corresponding spectrum. (c) Rotated rectangle, and (d) the corresponding spectrum. The spectrum corresponding to the translated rectangle is identical to the spectrum corresponding to the original image in Fig. 4.24(a).

Phase

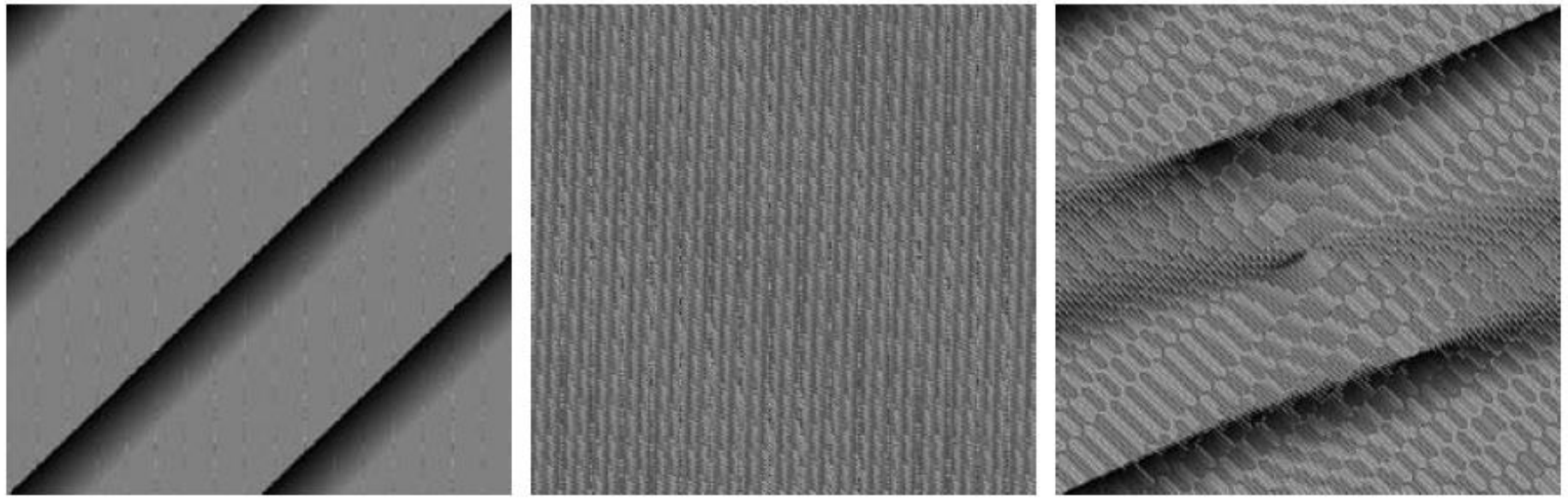

a b c

FIGURE 4.26 Phase angle array corresponding (a) to the image of the centered rectangle in Fig. 4.24(a), (b) to the translated image in Fig. 4.25(a), and (c) to the rotated image in Fig. 4.25(c).

Importance of Phase

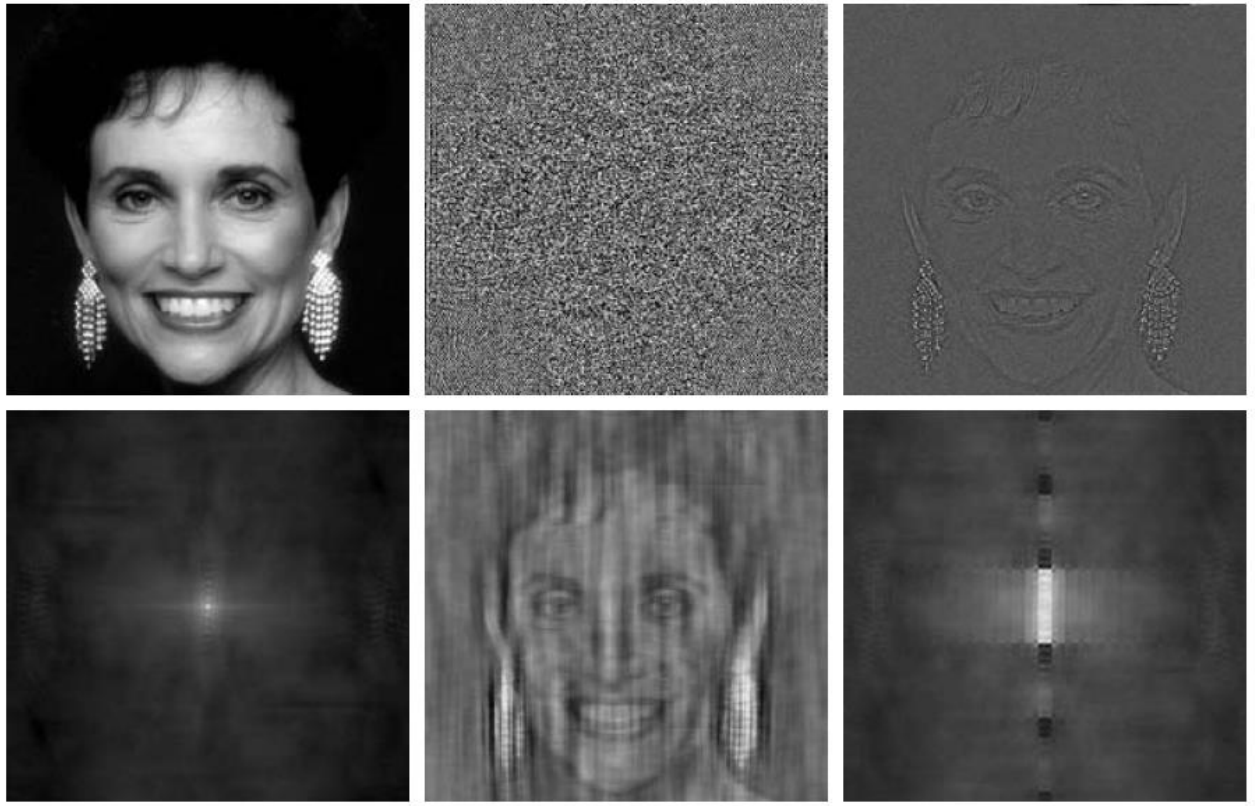

a b c
d e f

FIGURE 4.27 (a) Woman. (b) Phase angle. (c) Woman reconstructed using only the phase angle. (d) Woman reconstructed using only the spectrum. (e) Reconstruction using the phase angle corresponding to the woman and the spectrum corresponding to the rectangle in Fig. 4.24(a). (f) Reconstruction using the phase of the rectangle and the spectrum of the woman.

The 2-D Convolution Theorem

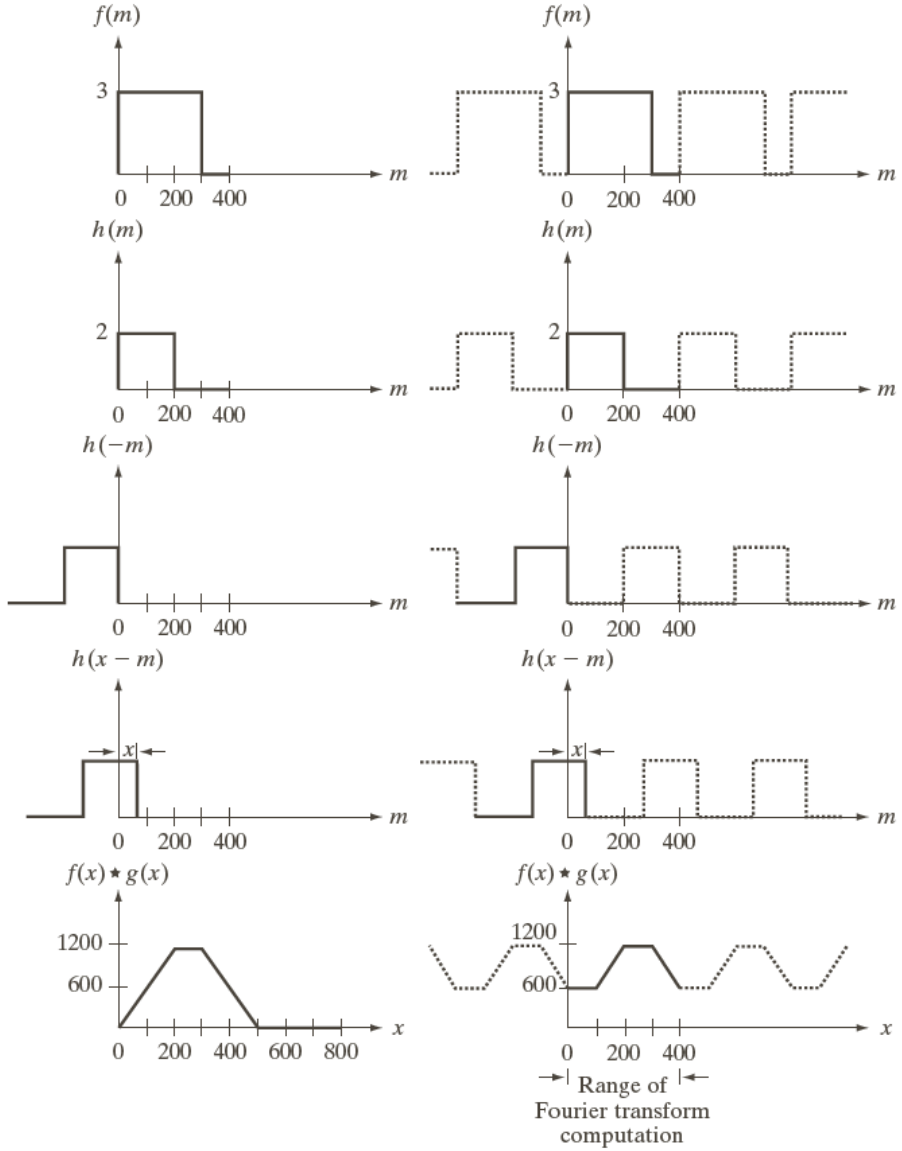

a f
b g
c h
d i
e j

FIGURE 4.28 Left column: convolution of two discrete functions obtained using the approach discussed in Section 3.4.2. The result in (e) is correct. Right column: Convolution of the same functions, but taking into account the periodicity implied by the DFT. Note in (j) how data from adjacent periods produce wraparound error, yielding an incorrect convolution result. To obtain the correct result, function padding must be used.

$$f(x) * h(x) = \sum_{m=0}^{399} f(m)\, h(x-m)$$

(i) Rotate h by 180°

(ii) Translate it by x

(iii) Sum of product.

x : 400 + 400 − 1 = 799.

"wrap around error"

$P \geq A + B - 1$ f(n) has length A.

h(n) " " B.

'Windowing' or 'apodizing' to address frequency leakage.

$[f(x,y)]_{A \times B}$ $\quad$ $[h(x,y)]_{C \times D}$.

$$f_p(x,y) = \begin{cases} f(x,y) & 0 \le x \le A-1 \text{ and } 0 \le y \le B-1 \\ 0 & A \le x \le P \text{ and } B \le y \le Q \end{cases}$$

$P \times Q$

$$h_p(x,y) = \begin{cases} h(x,y) & 0 \le x \le C-1 \text{ and } 0 \le y \le D-1 \\ 0 & C \le x < P \text{ and } D \le y \le Q. \end{cases}$$

$P \geq A+C-1$; $Q \geq B+D-1$

Summary of Definitions

Name	Expression(s)
1) Discrete Fourier transform (DFT) of $f(x, y)$	$F(u, v) = \sum_{x=0}^{M-1} \sum_{y=0}^{N-1} f(x, y) e^{-j2\pi(ux/M + vy/N)}$
2) Inverse discrete Fourier transform (IDFT) of $F(u, v)$	$f(x, y) = \frac{1}{MN} \sum_{u=0}^{M-1} \sum_{v=0}^{N-1} F(u, v) e^{j2\pi(ux/M + vy/N)}$
3) Polar representation	$F(u, v) = \lvert F(u, v) \rvert e^{j\phi(u,v)}$
4) Spectrum	$\lvert F(u, v) \rvert = \left[R^2(u, v) + I^2(u, v) \right]^{1/2}$ $R = \text{Real}(F); \quad I = \text{Imag}(F)$
5) Phase angle	$\phi(u, v) = \tan^{-1}\left[\frac{I(u, v)}{R(u, v)} \right]$
6) Power spectrum	$P(u, v) = \lvert F(u, v) \rvert^2$
7) Average value	$\overline{f}(x, y) = \frac{1}{MN} \sum_{x=0}^{M-1} \sum_{y=0}^{N-1} f(x, y) = \frac{1}{MN} F(0, 0)$

(Continued)

Name	Expression(s)
8) Periodicity (k_1 and k_2 are integers)	$F(u, v) = F(u + k_1 M, v) = F(u, v + k_2 N)$ $= F(u + k_1 M, v + k_2 N)$ $f(x, y) = f(x + k_1 M, y) = f(x, y + k_2 N)$ $= f(x + k_1 M, y + k_2 N)$
9) Convolution	$f(x, y) \star h(x, y) = \sum_{m=0}^{M-1} \sum_{n=0}^{N-1} f(m, n) h(x - m, y - n)$
10) Correlation	$f(x, y) \star h(x, y) = \sum_{m=0}^{M-1} \sum_{n=0}^{N-1} f^*(m, n) h(x + m, y + n)$
11) Separability	The 2-D DFT can be computed by computing 1-D DFT transforms along the rows (columns) of the image, followed by 1-D transforms along the columns (rows) of the result. See Section 4.11.1.
12) Obtaining the inverse Fourier transform using a forward transform algorithm.	$MNf^*(x, y) = \sum_{u=0}^{M-1} \sum_{v=0}^{N-1} F^*(u, v) e^{-j2\pi(ux/M + vy/N)}$ This equation indicates that inputting $F^*(u, v)$ into an algorithm that computes the forward transform (right side of above equation) yields $MNf^*(x, y)$. Taking the complex conjugate and dividing by MN gives the desired inverse. See Section 4.11.2.

Summary of Properties

Name	DFT Pairs
1) Symmetry properties	See Table 4.1
2) Linearity	$af_1(x, y) + bf_2(x, y) \Leftrightarrow aF_1(u, v) + bF_2(u, v)$
3) Translation (general)	$f(x, y)\, e^{j2\pi(u_0x/M + v_0y/N)} \Leftrightarrow F(u - u_0, v - v_0)$ $f(x - x_0, y - y_0) \Leftrightarrow F(u, v)e^{-j2\pi(ux_0/M + vy_0/N)}$
4) Translation to center of the frequency rectangle, $(M/2, N/2)$	$f(x, y)(-1)^{x+y} \Leftrightarrow F(u - M/2, v - N/2)$ $f(x - M/2, y - N/2) \Leftrightarrow F(u, v)(-1)^{u+v}$
5) Rotation	$f(r, \theta + \theta_0) \Leftrightarrow F(\omega, \varphi + \theta_0)$ $x = r\cos\theta \quad y = r\sin\theta \quad u = \omega\cos\varphi \quad v = \omega\sin\varphi$
6) Convolution theorem†	$f(x, y) \star h(x, y) \Leftrightarrow F(u, v)H(u, v)$ $f(x, y)h(x, y) \Leftrightarrow F(u, v) \star H(u, v)$

(Continued)

Name	DFT Pairs
7) Correlation theorem†	$f(x, y) \star h(x, y) \Leftrightarrow F^*(u, v)\, H(u, v)$ $f^*(x, y)h(x, y) \Leftrightarrow F(u, v) \star H(u, v)$
8) Discrete unit impulse	$\delta(x, y) \Leftrightarrow 1$
9) Rectangle	$\text{rect}[a, b] \Leftrightarrow ab\dfrac{\sin(\pi ua)}{(\pi ua)}\dfrac{\sin(\pi vb)}{(\pi vb)}e^{-j\pi(ua+vb)}$
10) Sine	$\sin(2\pi u_0x + 2\pi v_0y) \Leftrightarrow$ $j\dfrac{1}{2}\left[\delta(u + Mu_0, v + Nv_0) - \delta(u - Mu_0, v - Nv_0)\right]$
11) Cosine	$\cos(2\pi u_0x + 2\pi v_0y) \Leftrightarrow$ $\dfrac{1}{2}\left[\delta(u + Mu_0, v + Nv_0) + \delta(u - Mu_0, v - Nv_0)\right]$

The following Fourier transform pairs are derivable only for continuous variables, denoted as before by t and z for spatial variables and by μ and ν for frequency variables. These results can be used for DFT work by sampling the continuous forms.

12) *Differentiation* (The expressions on the right assume that $f(\pm\infty, \pm\infty) = 0$.)	$\left(\dfrac{\partial}{\partial t}\right)^m\left(\dfrac{\partial}{\partial z}\right)^n f(t, z) \Leftrightarrow (j2\pi\mu)^m(j2\pi\nu)^n F(\mu, \nu)$ $\dfrac{\partial^m f(t, z)}{\partial t^m} \Leftrightarrow (j2\pi\mu)^m F(\mu, \nu); \dfrac{\partial^n f(t, z)}{\partial z^n} \Leftrightarrow (j2\pi\nu)^n F(\mu, \nu)$
13) *Gaussian*	$A2\pi\sigma^2 e^{-2\pi^2\sigma^2(t^2+z^2)} \Leftrightarrow Ae^{-(\mu^2+\nu^2)/2\sigma^2}$ (A is a constant)

†Assumes that the functions have been extended by zero padding. Convolution and correlation are associative, commutative, and distributive.

Filtering in the Frequency Domain: Steps

- Given an input image $f(x, y)$ of size $M \times N$, obtain the padding parameters $P = 2M$ and $Q = 2N$.
- Form a padded image, $f_p(x, y)$, of size $P \times Q$ by adding necessary number of zeros to $f(x, y)$.
- Multiply $f_p(x, y)$ by $(-1)^{x+y}$ to centre its transform.
- Compute DFT of the image.
- Generate a real symmetric filter function, $H(u, v)$, of size $P \times Q$ with centre at coordinates $(P/2, Q/2)$
- Form the product $G(u, v) = H(u, v)F(u, v)$
- Obtain the processed image $g_p(x, y) = \{Re[\mathcal{F}^{-1}[G(u, v)]]\}(-1)^{x+y}$
- Obtain the final processed result, $g(x, y)$, by extracting $M \times N$ region from the top, left quadrant of $g_p(x, y)$.

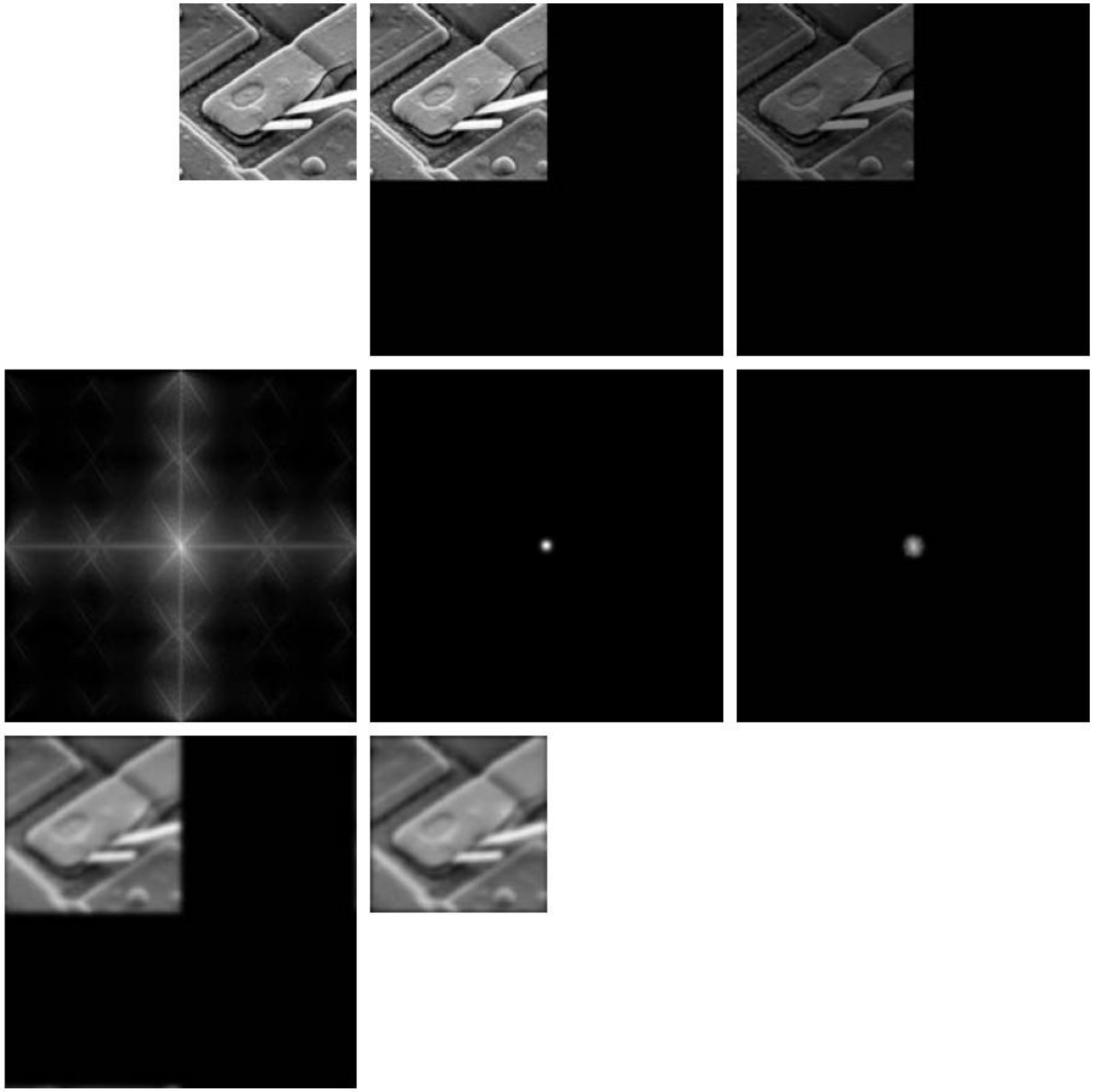

a b c
d e f
g h

FIGURE 4.36
(a) An $M \times N$ image, f.
(b) Padded image, f_p of size $P \times Q$.
(c) Result of multiplying f_p by $(-1)^{x+y}$.
(d) Spectrum of F_p. (e) Centered Gaussian lowpass filter, H, of size $P \times Q$.
(f) Spectrum of the product HF_p.
(g) g_p, the product of $(-1)^{x+y}$ and the real part of the IDFT of HF_p.
(h) Final result, g, obtained by cropping the first M rows and N columns of g_p.

Low Pass Filtering with Ideal filter

- $H(u,v) = \begin{cases} 1, & D(u,v) \le D_0 \\ 0, & D(u,v) > D_0 \end{cases}$

$$D(u,v) = \left[\left(u - \frac{P}{2}\right)^2 + \left(v - \frac{Q}{2}\right)^2\right]^{1/2}$$

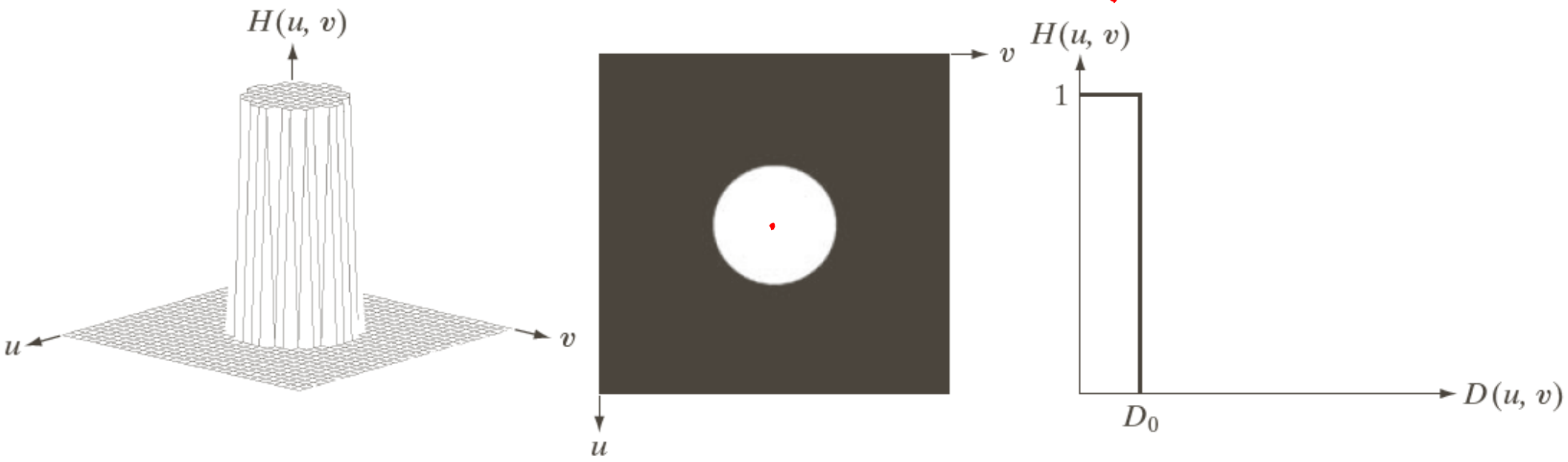

a b c

FIGURE 4.40 (a) Perspective plot of an ideal lowpass-filter transfer function. (b) Filter displayed as an image. (c) Filter radial cross section.

Results

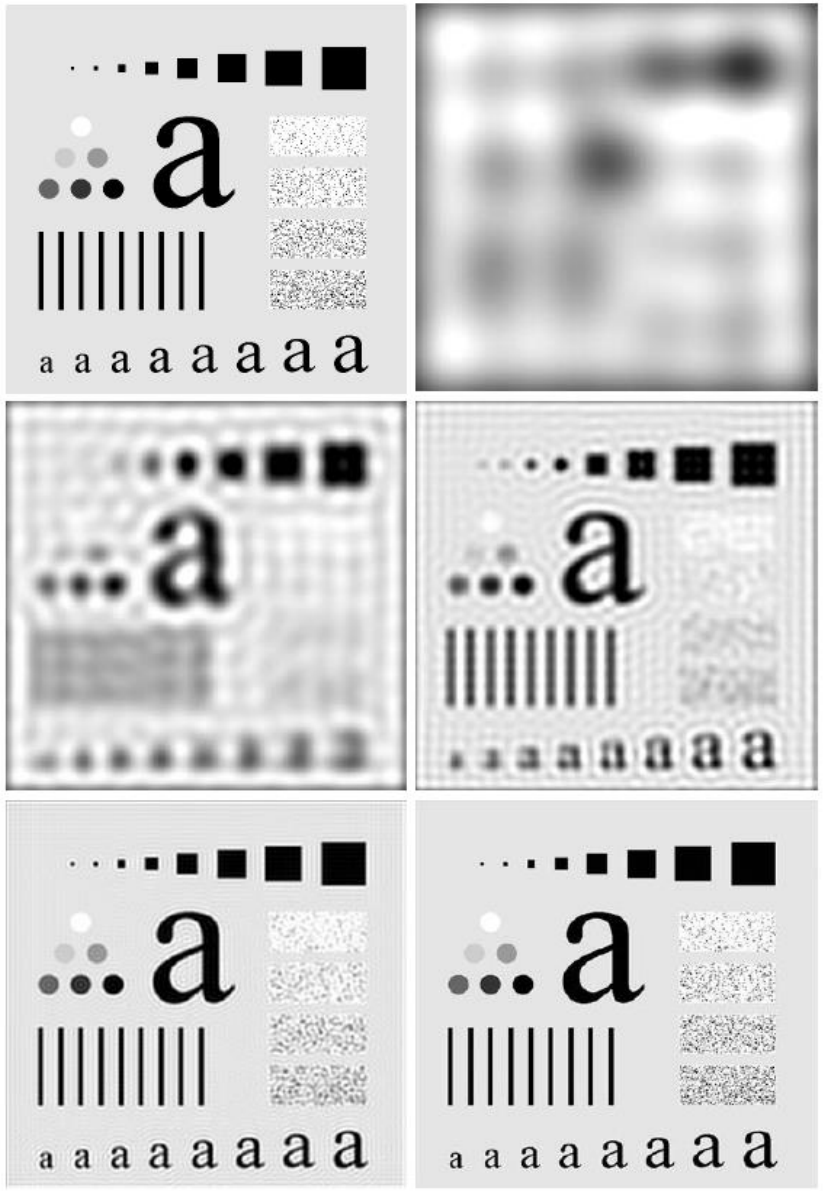

a b
c d
e f

FIGURE 4.42 (a) Original image. (b)–(f) Results of filtering using ILPFs with cutoff frequencies set at radii values 10, 30, 60, 160, and 460, as shown in Fig. 4.41(b). The power removed by these filters was 13, 6.9, 4.3, 2.2, and 0.8% of the total, respectively.

Ringing artifacts.

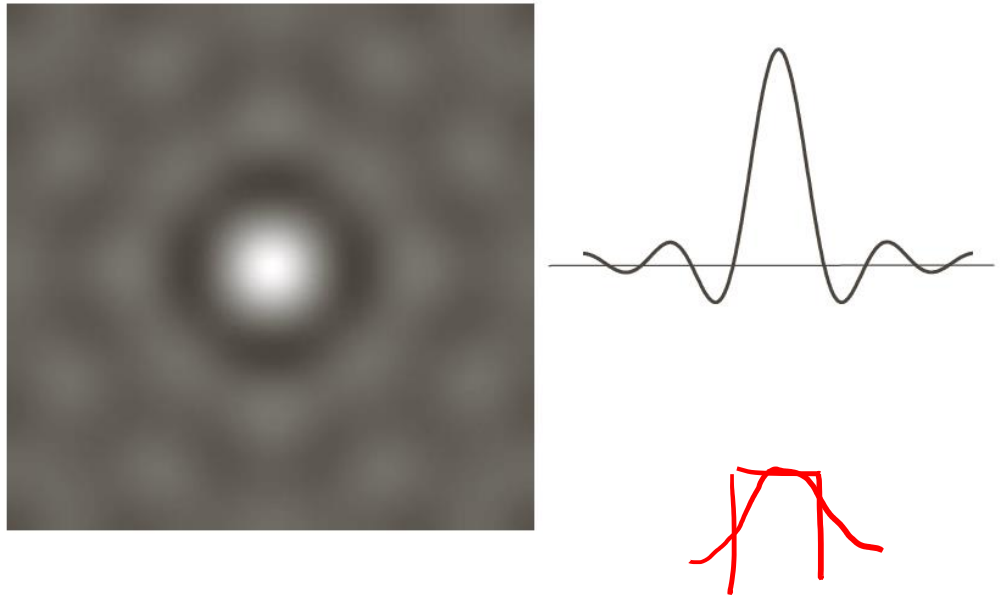

a b

FIGURE 4.43 (a) Representation in the spatial domain of an ILPF of radius 5 and size 1000 × 1000. (b) Intensity profile of a horizontal line passing through the center of the image.

Butterworth Lowpass Filters

- $H(u,v) = \dfrac{1}{1+[D(u,v)/D_0]^{2n}}$ $\quad D(u,v) = \left[\left(u - \dfrac{P}{2}\right)^2 + \left(v - \dfrac{q}{2}\right)^2\right]^{1/2}$

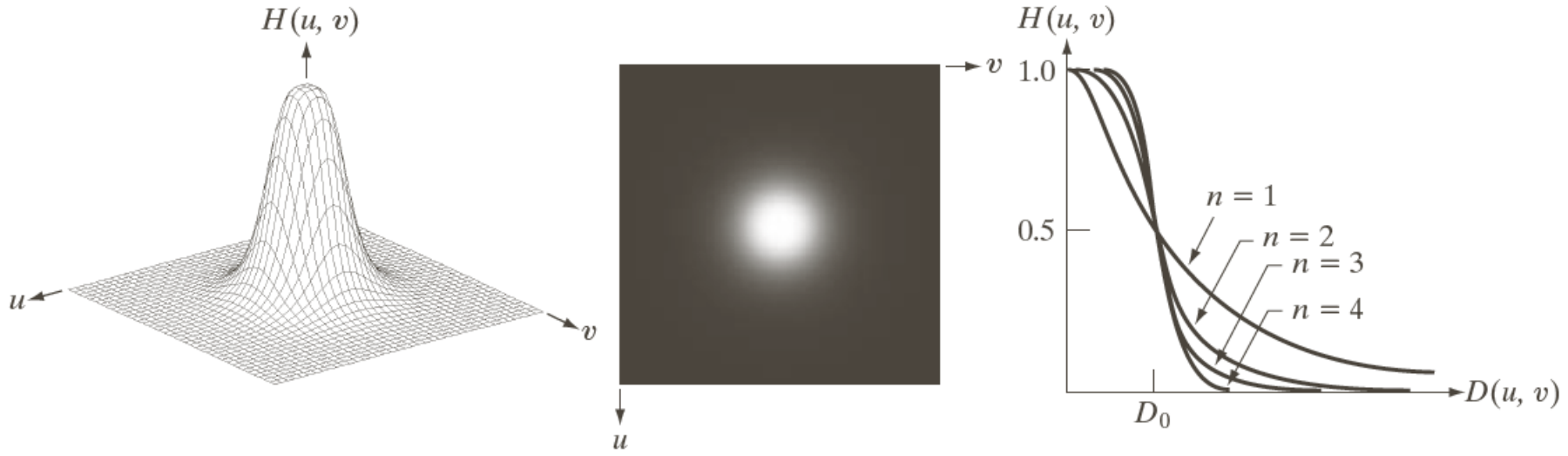

a b c

FIGURE 4.44 (a) Perspective plot of a Butterworth lowpass-filter transfer function. (b) Filter displayed as an image. (c) Filter radial cross sections of orders 1 through 4.

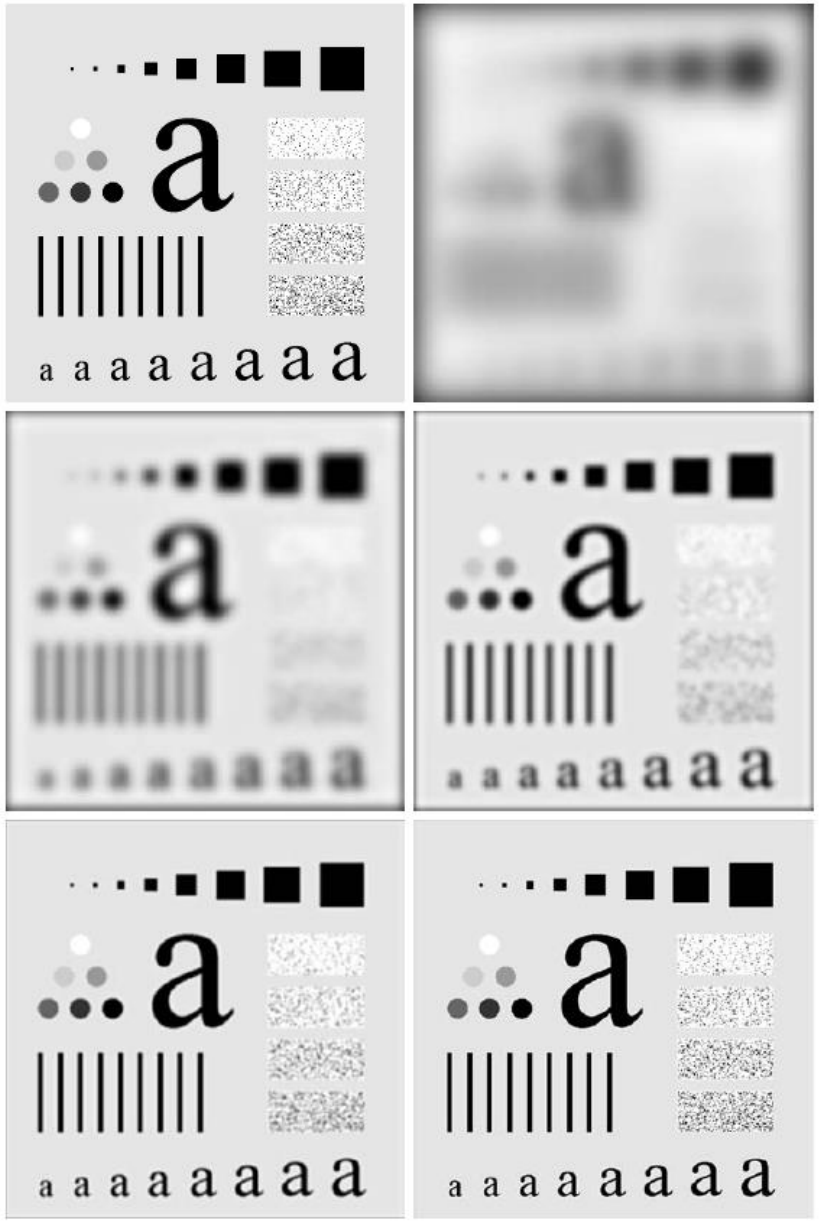

a b
c d
e f

FIGURE 4.45 (a) Original image. (b)–(f) Results of filtering using BLPFs of order 2, with cutoff frequencies at the radii shown in Fig. 4.41. Compare with Fig. 4.42.

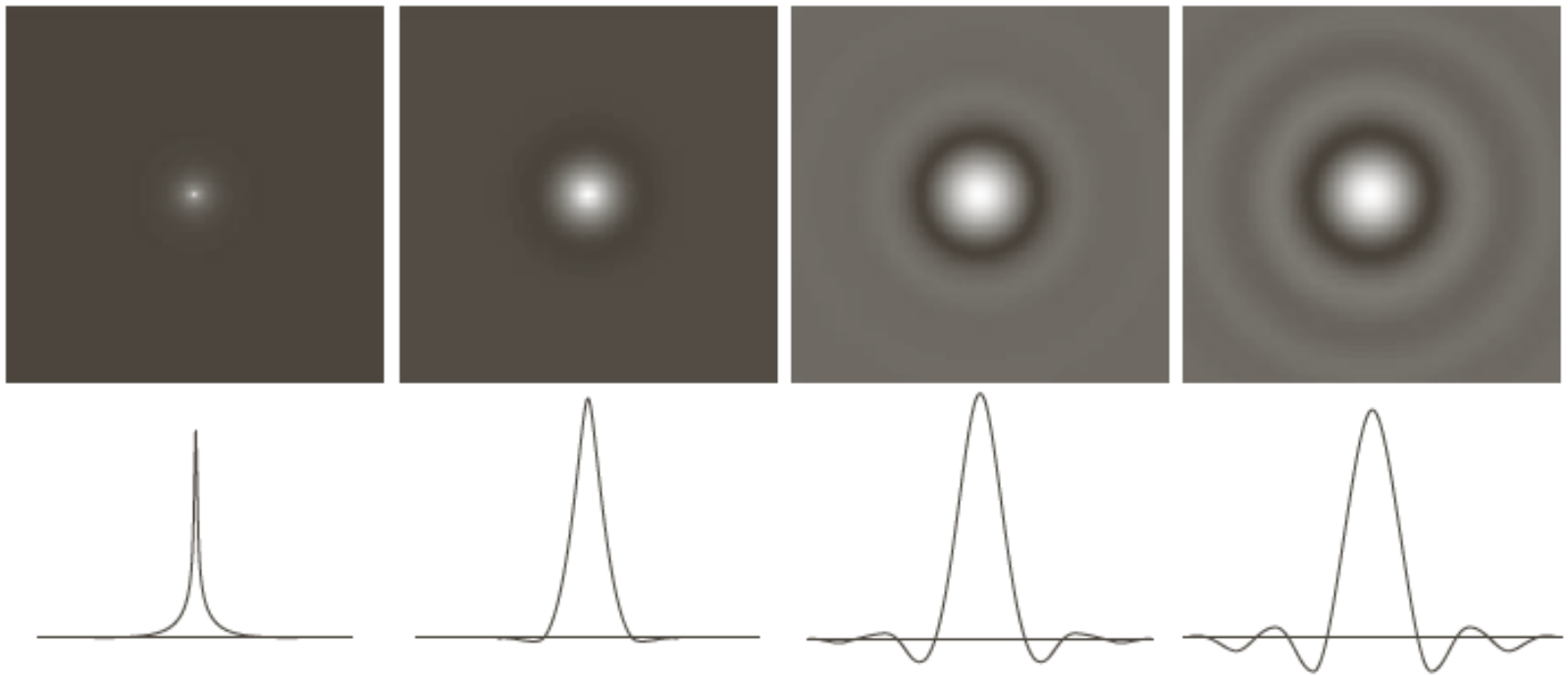

a b c d

FIGURE 4.46 (a)–(d) Spatial representation of BLPFs of order 1, 2, 5, and 20, and corresponding intensity profiles through the center of the filters (the size in all cases is 1000 × 1000 and the cutoff frequency is 5). Observe how ringing increases as a function of filter order.

Gaussian Lowpass Filters

- $H(u,v) = e^{-D^2(u,v)/2\sigma^2}$ $H(u,v) = e^{-D^2(u,v)/2D_0^2}$

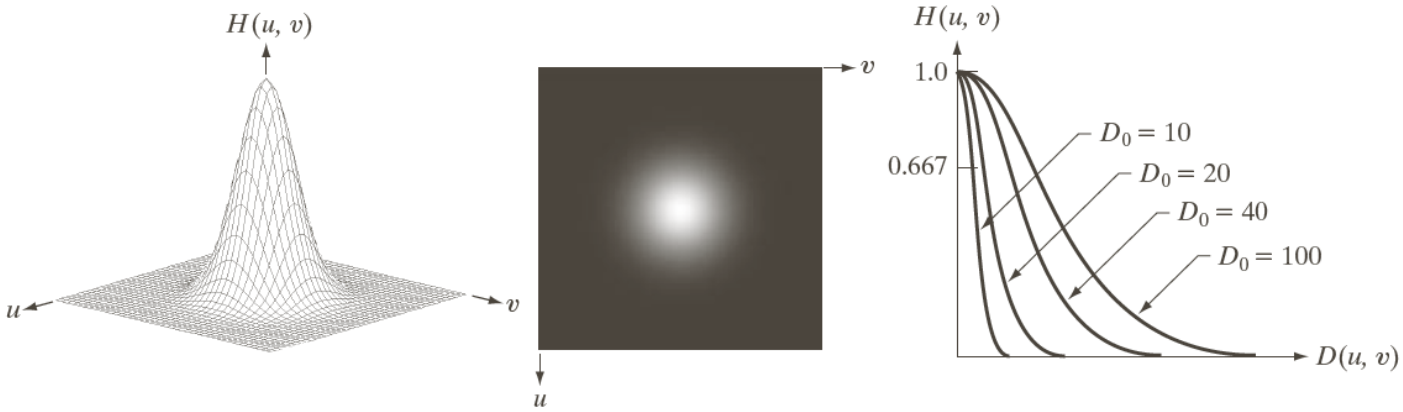

a b c

FIGURE 4.47 (a) Perspective plot of a GLPF transfer function. (b) Filter displayed as an image. (c) Filter radial cross sections for various values of D_0.

TABLE 4.4

Lowpass filters. D_0 is the cutoff frequency and n is the order of the Butterworth filter.

Ideal	Butterworth	Gaussian
$H(u,v) = \begin{cases} 1 & \text{if } D(u,v) \le D_0 \\ 0 & \text{if } D(u,v) > D_0 \end{cases}$	$H(u,v) = \dfrac{1}{1 + [D(u,v)/D_0]^{2n}}$	$H(u,v) = e^{-D^2(u,v)/2D_0^2}$

Results

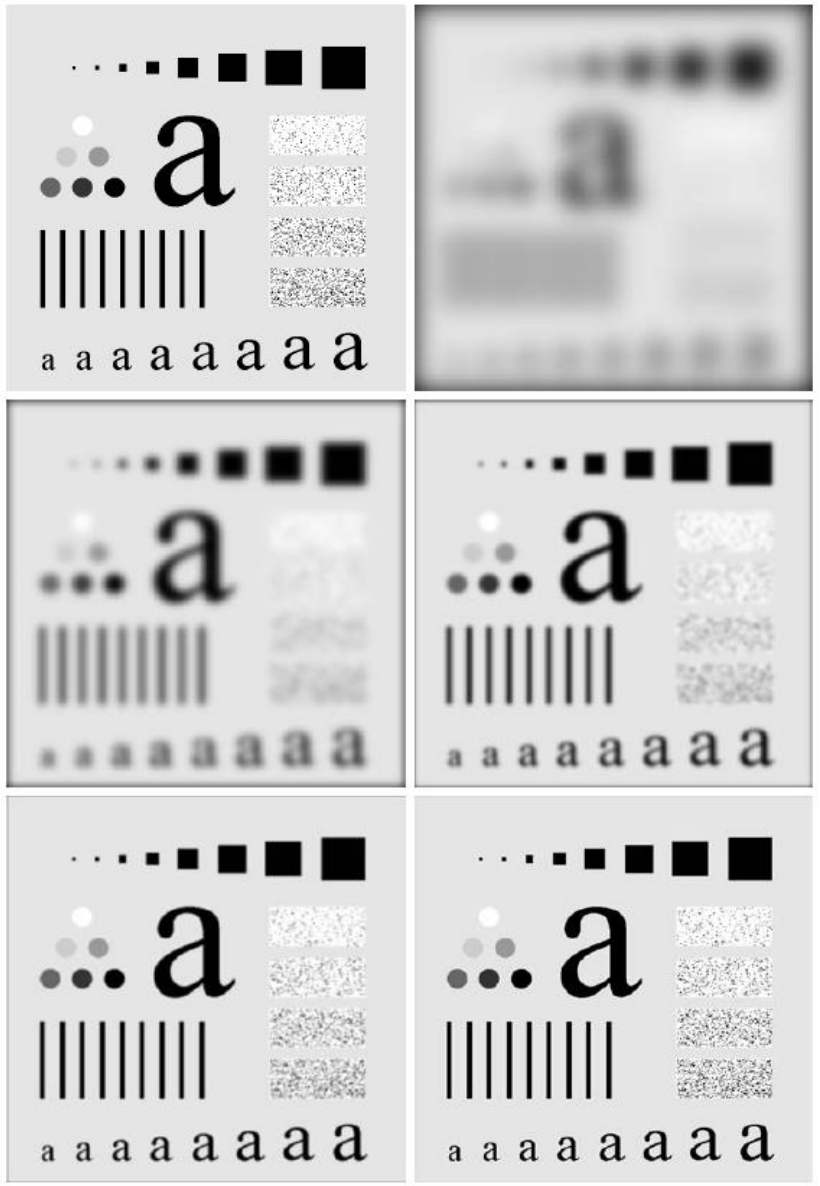

a b
c d
e f

FIGURE 4.48 (a) Original image. (b)–(f) Results of filtering using GLPFs with cutoff frequencies at the radii shown in Fig. 4.41. Compare with Figs. 4.42 and 4.45.

Results

a b c

FIGURE 4.50 (a) Original image (784 × 732 pixels). (b) Result of filtering using a GLPF with $D_0 = 100$. (c) Result of filtering using a GLPF with $D_0 = 80$. Note the reduction in fine skin lines in the magnified sections in (b) and (c).

Results

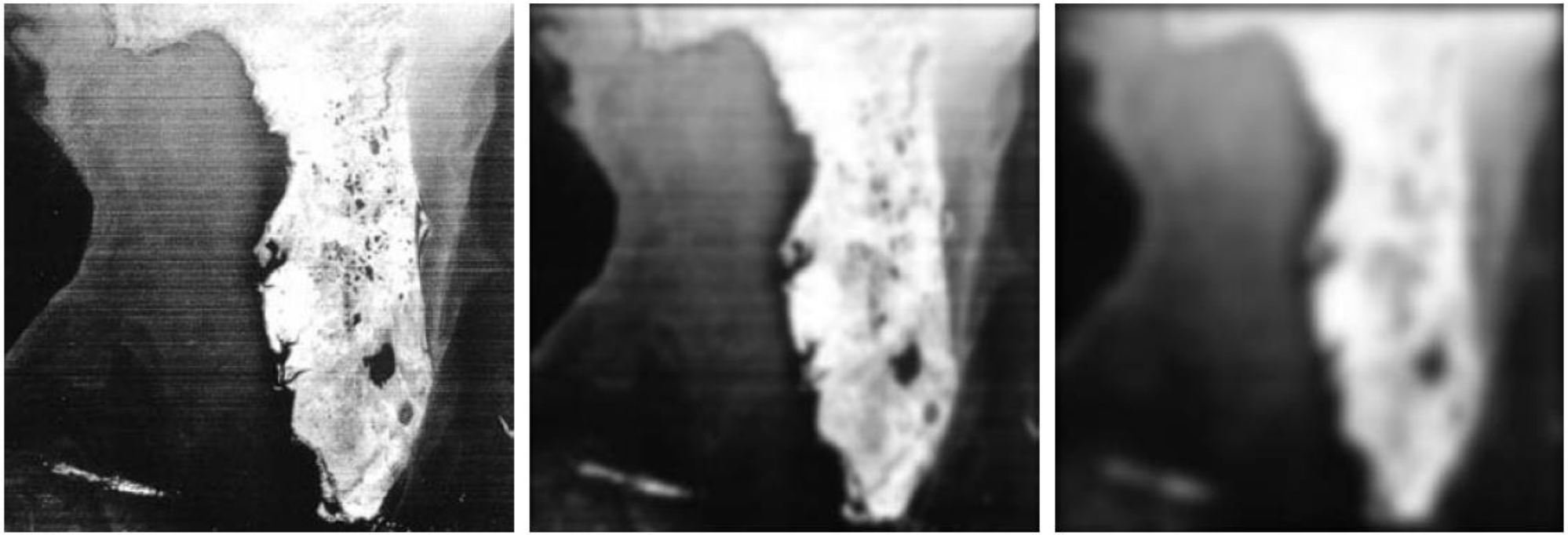

a b c

FIGURE 4.51 (a) Image showing prominent horizontal scan lines. (b) Result of filtering using a GLPF with $D_0 = 50$. (c) Result of using a GLPF with $D_0 = 20$. (Original image courtesy of NOAA.)

Image Sharpening Using Frequency Domain Filters

- $H_{HP}(u,v) = 1 - H_{LP}(u,v)$

TABLE 4.5
Highpass filters. D_0 is the cutoff frequency and n is the order of the Butterworth filter.

Ideal	Butterworth	Gaussian
$H(u,v) = \begin{cases} 0 & \text{if } D(u,v) \le D_0 \\ 1 & \text{if } D(u,v) > D_0 \end{cases}$	$H(u,v) = \dfrac{1}{1 + [D_0/D(u,v)]^{2n}}$	$H(u,v) = 1 - e^{-D^2(u,v)/2D_0^2}$

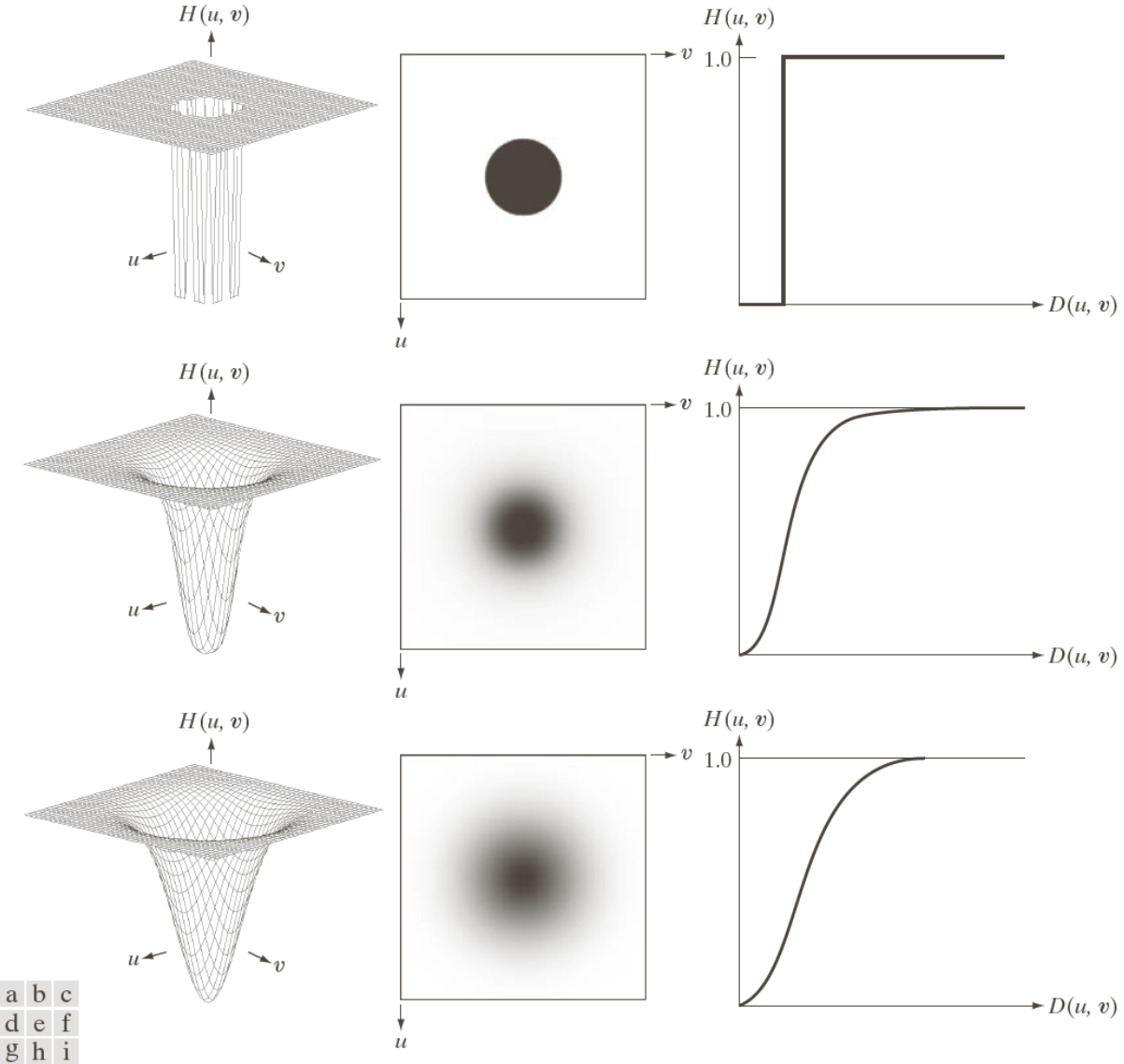

FIGURE 4.52 Top row: Perspective plot, image representation, and cross section of a typical ideal highpass filter. Middle and bottom rows: The same sequence for typical Butterworth and Gaussian highpass filters.

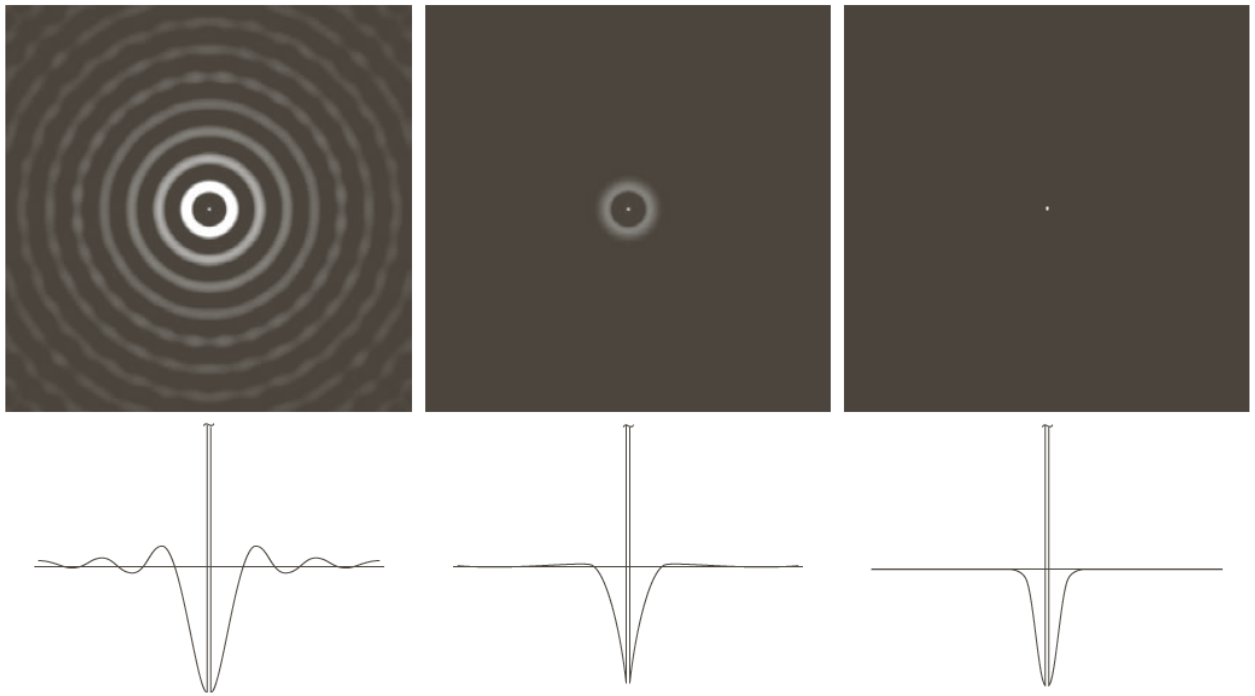

FIGURE 4.53 Spatial representation of typical (a) ideal, (b) Butterworth, and (c) Gaussian frequency domain highpass filters, and corresponding intensity profiles through their centers.

Results of IHPF

a b c

FIGURE 4.54 Results of highpass filtering the image in Fig. 4.41(a) using an IHPF with $D_0 = 30$, 60, and 160.

Results of BHPF

a b c

FIGURE 4.55 Results of highpass filtering the image in Fig. 4.41(a) using a BHPF of order 2 with $D_0 = 30, 60,$ and 160, corresponding to the circles in Fig. 4.41(b). These results are much smoother than those obtained with an IHPF.

Results of GHPF

a b c

FIGURE 4.56 Results of highpass filtering the image in Fig. 4.41(a) using a GHPF with $D_0 = 30$, 60, and 160, corresponding to the circles in Fig. 4.41(b). Compare with Figs. 4.54 and 4.55.

Laplacian in Frequency Domain

$f(x,y) + \nabla^2 f(x,y)$

$H(u,v) = -4\pi^2(u^2+v^2) \Rightarrow -4\pi^2\left[(u-P/2)^2 + (v-Q/2)^2\right]$

$= -4\pi D^2(u,v)$

$\mathcal{F}^{-1}[F(u,v)H(u,v)]$

$= \nabla^2 f(x,y)$

a b

FIGURE 4.58
(a) Original, blurry image. (b) Image enhanced using the Laplacian in the frequency domain. Compare with Fig. 3.38(e).

$\mathcal{F}^{-1}\{F(u,v) - H(u,v)F(u,v)\}$

$= \mathcal{F}^{-1}\{[1 + 4\pi^2 D^2(u,v)]F(u,v)\}$.

$$g_{mask} = f(x,y) - \bar{f}(x,y)$$

$$\bar{f}(x,y) = \mathcal{F}^{-1}\{H_{LP}(u,v)\,F(u,v)\}$$

$$\hat{f}(x,y) = f(x,y) + k * g_{mask}$$

$k = 1$ unsharp masking

$k > 1$ high boost filtering.

$$\hat{f}(x,y) = \mathcal{F}^{-1}\{[1 + k * [1 - H_{LP}(u,v)]]\,F(u,v)\}.$$

Homomorphic Filtering

FIGURE 4.60
Summary of steps in homomorphic filtering.

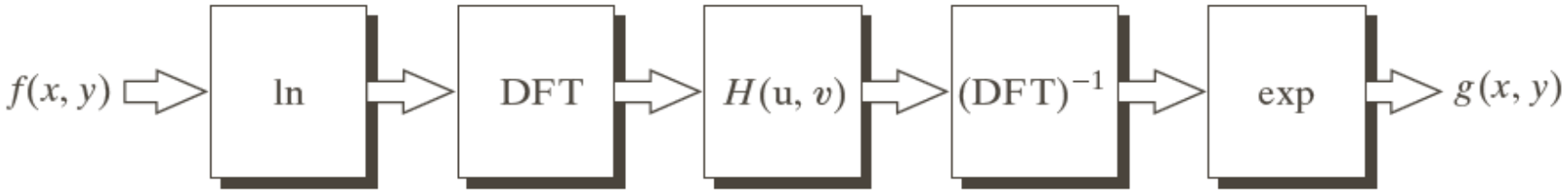

$f(x,y) = i(x,y) \cdot r(x,y)$

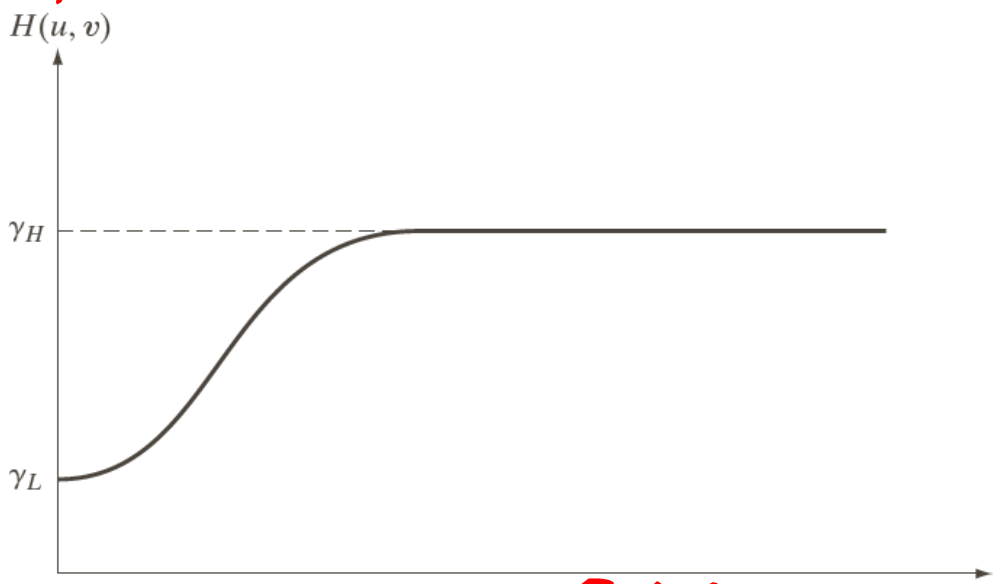

FIGURE 4.61
Radial cross section of a circularly symmetric homomorphic filter function. The vertical axis is at the center of the frequency rectangle and $D(u, v)$ is the distance from the center.

$H(u,v) = (\gamma_H - \gamma_L)\left[1 - e^{-c[D^2(u,v)/D_0^2]}\right] + \gamma_L$

$$f(x,y) = i(x,y)\, r(x,y) \qquad \mathcal{F}[f(x,y)] \neq \mathcal{F}[i(x,y)]\,\mathcal{F}[r(x,y)]$$

$$z(x,y) = \ln f(x,y) = \ln i(x,y) + \ln r(x,y)$$

$$\mathcal{F}[z(x,y)] = \mathcal{F}[\ln i(x,y)] + \mathcal{F}[\ln r(x,y)].$$

$$Z(u,v) = I(u,v) + R(u,v)$$

$$S(u,v) = H(u,v)\,Z(u,v) = H(u,v)\,I(u,v) + H(u,v)\,R(u,v)$$

$$\mathcal{F}^{-1}[S(u,v)] = \underbrace{\mathcal{F}^{-1}\{H(u,v)\,I(u,v)\}}_{i'(x,y)} + \underbrace{\mathcal{F}^{-1}\{H(u,v)\,R(u,v)\}}_{r'(x,y)}.$$

$$s(x,y) = i'(x,y) + r'(x,y)$$

$$e^{s(x,y)} = e^{i'(x,y)} \cdot e^{r'(x,y)}$$

$$g(x,y) = i_0(x,y)\, r_0(x,y)$$

Results

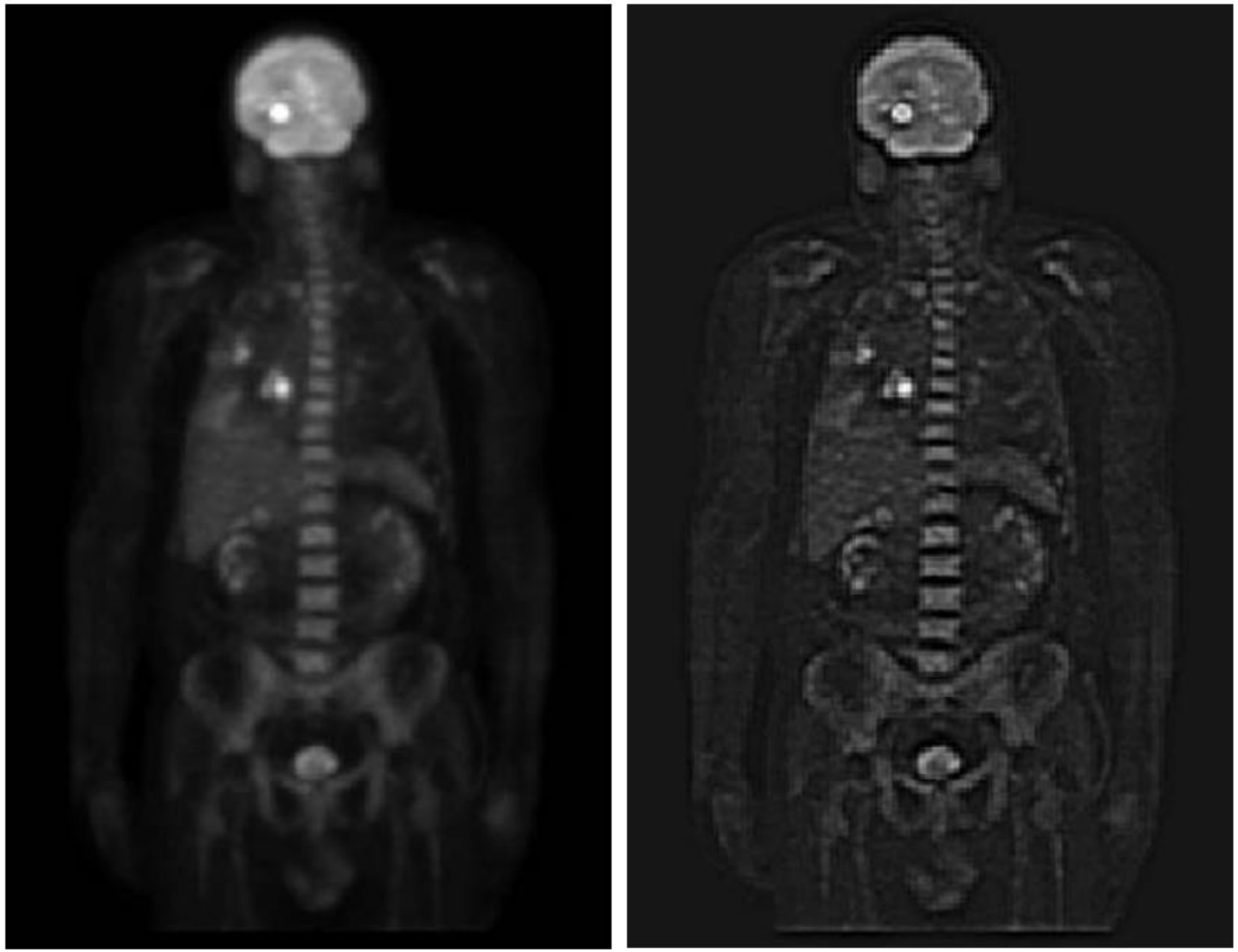

a b

FIGURE 4.62
(a) Full body PET scan. (b) Image enhanced using homomorphic filtering. (Original image courtesy of Dr. Michael E. Casey, CTI PET Systems.)